Tribology International 126 (2018) 186–191

Contents lists available at ScienceDirect

Tribology International

journal homepage: www.elsevier.com/locate/triboint

Boundary layers: Unifying the impact and rolling EHL point contacts

A.A. Lubrecht[a,*], N. Biboulet[a], C.H. Venner[b]

[a] Université de Lyon, INSA-Lyon, LaMCoS, CNRS UMR 5259, Villeurbanne, F69621, France
[b] Universiteit Twente, Enschede, the Netherlands

ARTICLE INFO

Keywords:
EHL
Impact lubrication
Amplitude reduction theory

ABSTRACT

Transient effects in elastohydrodynamic lubrication occur due to varying operating conditions and surface features moving through the contact. For rolling/sliding contacts the lubricated contact behaviour is determined by a unifying mechanism characterized by the inlet length (boundary layer). Roughness deformation depends on a single dimensionless parameter representing the ratio inlet length to wavelength. This behaviour is shown to generalize to the pure impact problem. The bell shaped film thickness near the periphery of the contact is directly related to the boundary layer velocity profile. Also, the waviness deformation under impact conditions is shown to depend on the same parameter as in rolling contacts when the rolling velocity is replaced by the local boundary layer velocity in the impact problem.

1. Introduction

Lubricated concentrated contacts as appearing between gear teeth, in rolling bearings and cam-follower mechanisms have now been studied for over 100 years. Martin [1] and Gümbel [2] showed that standard lubrication theory is unable to predict sufficient lubricant film formation to separate surfaces with realistic roughness. The two missing physical effects explaining lubrication are the elastic deformation of the surfaces and the viscosity pressure dependence as was demonstrated by Ertel and Grubin [3]. The viscosity pressure dependence introduces the special feature of a pressure spike, first shown in the solutions presented by Petrusevich [4]. Hence, lubrication of concentrated contacts was established as a separate specialism: ElastoHydrodynamical Lubrication. Based on numerical solutions, film thickness predictions were derived for line contact by Dowson and Higginson [5] and for circular contact by Hamrock and Dowson [6]. Both formulas are still widely used. The development of faster, more stable and efficient numerical algorithms and the advances in computer hardware in terms of computational speed and memory capacity, have led to the study of increasingly complex and realistic problems. Since the late 1980's many theoretical studies by different groups of researchers have appeared leading to a very advanced understanding of film thickness behaviour under steady state (isothermal) fully flooded conditions, e.g. see Ref. [7] (and later [8–10]), under starved conditions [11], in transient problems of varying load and speed [12–14] and with surface features moving through the contact, [15,16]. Several authors simulated measured surface roughness profiles in point contacts moving through the contact and many other phenomena, e.g. see Ref. [17]. As an alternative to the simulations with measured roughness proflies, a group of researchers developed a conceptual approach to derive an engineering relation for roughness deformation from the study of the deformation of harmonic waviness, e.g. see Refs. [18–22]. It was found that the deformation was governed by a unifying mechanism reflected by a single nondimensional parameter representing the ratio of inlet length to wavelength which was shown to generalize for all contacts including starved ones [23]. The physical rationale and generality for line and point contacts (isoviscous) is presented in Ref. [44]. As a result of the many studies rolling/sliding EHL contacts are well understood. Many of the phenomena observed have been validated experimentally using optical interferometry with a model ball on disc contact [24]. Overviews of the many developments can be found in Refs. [25–27].

The problem of two bodies in normal approach, referred to as the impact EHL contact has received much less attention. The dry contact impact problem is described by Johnson [28]. Early numerical studies of the lubricated contact are found in the work of Christensen [29], Yang et al. [30] and Larsson et al. [31]. Detailed aspects were further analysed by Guo, Kaneta and Wang [32,33,35], and e.g. surface waviness effects in Ref. [34]. Experimental work includes that of Cameron [36], Safa [37], Wong [38] and Kaneta et al. [39,40]. In addition to the engineering literature, problems very similar to the impact problem are extensively discussed in the literature of physics, with relevance to, e.g. droplet impact, bubble interaction, and impact of soft materials e.g. see Ref. [41].

Under impact conditions when the two surfaces approach, lubricant is pushed to the sides and the pressure in the center increases as would be the case for undeformable surfaces. However, enhanced by the viscosity pressure dependence, the surfaces start to deform in the

* Corresponding author.
E-mail address: Ton.Lubrecht@insa-lyon.fr (A.A. Lubrecht).

https://doi.org/10.1016/j.triboint.2018.05.019
Received 4 January 2018; Received in revised form 4 May 2018; Accepted 10 May 2018
Available online 12 May 2018
0301-679X/

Notation

a	Hertzian contact radius
a^*	maximum Hertzian contact radius (over time)
A_d	deformed waviness amplitude
A_i	initial waviness amplitude
E'	reduced elastic modulus
h	film thickness
H	dimensionless film thickness (Hertz) $H = hR/a^{*2}$
L	Moes parameter $L = \overline{\alpha}(\overline{\lambda}\pi^3/6)^{1/4}$
m	sphere mass
M	Moes parameter $M = ((128\pi^3)/(3\overline{\lambda}))^{1/4}$
P	pressure
p_h^*	maximum Hertzian pressure (over time)
P	dimensionless pressure $P = p/p_h^*$
R	reduced radius of curvature
$\mathcal{R}$	surface roughness (waviness)
t	time
t_0	impact or transit time $t_0 = \delta^*/v_0$ or $t_0 = a/u_m$
T	dimensionless time $T = t/t_0$
x	coordinate
X	dimensionless coordinate $X = x/a^*$
u_m	mean rolling velocity
v_0	initial vertical impact velocity
α	pressure viscosity index
$\overline{\alpha}$	product of pressure and viscosity index $\overline{\alpha} = \alpha p_h^*$
δ	Hertzian deformation a^2/R_x
δ^*	maximum Hertzian deformation a^{*2}/R_x
Δ	dimensionless deformation
η	viscosity, η_0 at ambient pressure
λ	waviness wavelength
$\overline{\lambda}$	dimensionless parameter $\overline{\lambda} = (12\eta_0 R^2)/(a^{*2}t_0 p_h^*)$
ρ	density, ρ_0 at ambient pressure

center, creating a bell shaped enclosure, entrapping lubricant. Subsequently, the minimum film thickness occurs near the sides where a thin film thickness front is advancing as the load and thereby the contact region, increases. The film shape in the periphery of the contact exhibits similar phenomena to the film thickness in the exit region of rolling/sliding contacts. During further impact the film thickness in the center changes only marginally. Upon rebound this remains to be the case and the thin film front at the periphery recedes. The film thickness in the center again remains roughly unchanged. In recent work the authors [42,43] generalised the film thickness prediction of the impact *central film thickness* for the Iso-Viscous Elastic and the Piezo-Viscous Elastic regimes for both line and point contacts. In these papers the behaviour of the film thickness in the region of minimum film thickness, i.e. the periphery of the contact is addressed. For rolling-sliding EHL contacts, it was shown that the film thickness is determined by the inlet pressure sweep (boundary layer), or in fact the transition region in which the importance of the Poiseuille flow terms decreases and shear flow starts to dominate. This boundary layer, its scaling, and the effect on the EHL film are described in Refs. [44–46]. The current work extends this boundary layer analysis to the film thickness behaviour in the impact problem. In particular it is shown that the waviness deformation under impact conditions, to a good approximation, is governed by the same mechanism as waviness amplitude reduction in the rolling contact problem.

To allow the reader to relate the operating conditions to the rolling/sliding contact, the Moes parameters [47,48] M and L are used. However, the authors are thoroughly convinced that the parameter set $(\overline{\alpha}, \overline{\lambda})$ is a more coherent choice as it seamlessly combines line and point contacts [8] as well as rolling/sliding and impacting contacts.

2. Theory

Consider the case of a ball impacting a flat with the two surfaces separated by a lubricant film, under the assumption of a thin layer flow, the Reynolds equation can be used. Using the parameters of the dry contact impact problem, see Ref. [43] the resulting dimensionless Reynolds equation is:

$$\frac{\partial}{\partial X}\left(\frac{\overline{\rho}H^3}{\overline{\eta}\overline{\lambda}}\frac{\partial P}{\partial X}\right) + \frac{\partial}{\partial Y}\left(\frac{\overline{\rho}H^3}{\overline{\eta}\overline{\lambda}}\frac{\partial P}{\partial Y}\right) - \frac{\partial(\overline{\rho}H)}{\partial T} = 0 \tag{1}$$

where

$$\overline{\lambda} = \frac{12\eta_0 R^3 v_0}{a^{*4} p_h^*} \tag{2}$$

in which a^* and p_h^* are the Hertzian contact radius and maximum Hertzian pressure at the moment of maximum impact in the dry contact impact case.

The viscosity and density pressure dependence have been modeled using the empirical relations presented by Roelands [49] and by Dowson and Higginson [5].

The equation for the dimensionless film thickness is:

$$H = -\Delta + \frac{X^2}{2} + \frac{Y^2}{2} - \mathcal{R}(X, Y) + \frac{2}{\pi^2}\int\int_S \frac{P(X', Y', T)\, dX'dY'}{\sqrt{(X - X')^2 + (Y - Y')^2}} \tag{3}$$

where Δ is the non dimensional mutual approach of two points in the solids which is determined by the Newton's second law for the impacting ball:

$$\frac{d^2\Delta}{dT^2} + \frac{3}{2\pi}\int_S P(X, Y)dXdY = 0 \tag{4}$$

The dimensionless initial conditions are:

$$\frac{d\Delta}{dT} = V_0 \tag{5}$$

and $\Delta(T = 0) = \Delta_0$.

The equations were discretized on a uniform grid with second order accuracy in space and (implicit) in time. The discrete equations at each time were solved using Multigrid techniques [13,43,50,51].

In the dimensionless rolling EHL contact the $\overline{\lambda}$ parameter reads:

$$\overline{\lambda} = \frac{12\eta_0 u_m R^2}{a^3 p_h} \tag{6}$$

In order to create the same $\overline{\lambda}$ parameter for the impact problem and the rolling problem one introduces the transport time t_0:

$$\overline{\lambda} = \frac{12\eta_0 u_m R^2}{a a^2 p_h} \tag{7}$$

$$\overline{\lambda} = \frac{12\eta_0 R^2}{t_0 a^2 p_h} \tag{8}$$

$$t_0 = a/u_m \tag{9}$$

Now the impact $\overline{\lambda}$ can be written in a similar way:

$$\overline{\lambda} = \frac{12\eta_0 R^3 v_0}{a^4 p_h} \tag{10}$$

$$\overline{\lambda} = \frac{12\eta_0 R^2 R v_0}{a^2 a^2 p_h} \tag{11}$$

$$\overline{\lambda} = \frac{12\eta_0 R^2}{t_0 a^2 p_h} \tag{12}$$

$$t_0 = \frac{\delta}{v_0} = \frac{a^2}{Rv_0} \quad \text{(Hertz)} \tag{13}$$

Now the impact time t_0 represents the ratio of the impact distance (the maximum Hertzian deformation δ^*) and the impact velocity v_0. Johnson [28] gives this impact time as 2.94, (see appendix).

This means that the lubricated impact problem and the rolling contact problem are described by the same Reynolds equation.

3. Impact velocity

Whereas the boundary layer horizontal velocity is constant in the rolling contact, it varies from close to infinity to zero during impact, depending on the operating conditions (especially the load condition).

The dry impact problem can once again be used as an important asymptotic solution. Simplifying Johnson's [28] approximate solution, the contact radius a varies with the contact time t as (see appendix):

$$\frac{a(t)}{a^*} = \sqrt{1 - \frac{t^2}{t^{*2}}} \tag{14}$$

with contact occurring for $t \in [-t^*, t^*]$.

In the following figures $t^* = 2.7$ and the time origin has been shifted to fit the dry contact problem.

Fig. 1 shows the evolution of the contact radius and its derivative as a function of time.

The (horizontal) velocity shows two vertical asymptotes, one at the first instant of impact and one at the last instant of impact. These two asymptotes find their origins in the infinite slopes of the Hertzian contact. Another interesting feature is the near-linear velocity evolution around maximum impact (see Appendix). Fig. 2 shows that this feature of the dry impact carries over to all sufficiently loaded lubricated impacts. This figure only shows the first half of the impact as this determines the film build-up.

If one uses the classical Hamrock and Dowson [6] relation between velocity and film thickness $h \propto u^{0.67}$ one can draw a “simplistic” theoretical film thickness prediction, see Fig. 3.

One can observe, especially from the zoomed Fig. 4, that the fit is not perfect, but the $h \propto u^{0.67}$ gives a very nice first order approximation of the film thickness shape for $0.75 < X < 0.95$. The film thickness in the central zone is created by the impact motion generating enough pressure for the oil to enter the piezo-viscous regime and be ”frozen” in the typical bell shape. This regime can obviously not be approximated by classical rolling sliding motion.

Having shown that the boundary layer velocity gives a good film thickness prediction, it is now time to analyse another aspect of the inlet boundary layer: the waviness amplitude reduction.

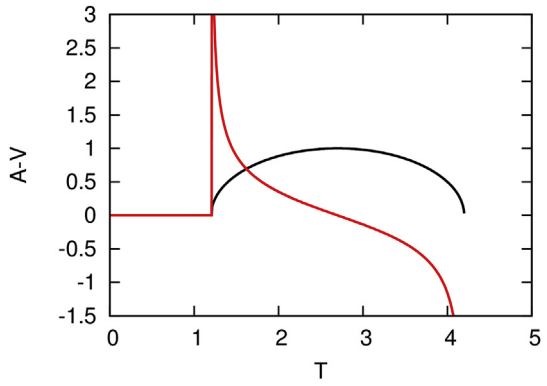

Fig. 1. Asymptotic (dry) impact analysis, contact radius a/a^* (black) and radius velocity v/v^* (red). (For interpretation of the references to colour in this figure legend, the reader is referred to the Web version of this article.)

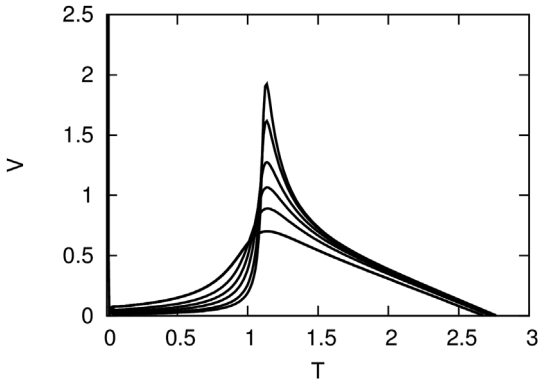

Fig. 2. Lubricated impact analysis, contact radius velocity for $M = 200 - 10000$ (left to right), $L = 10$.

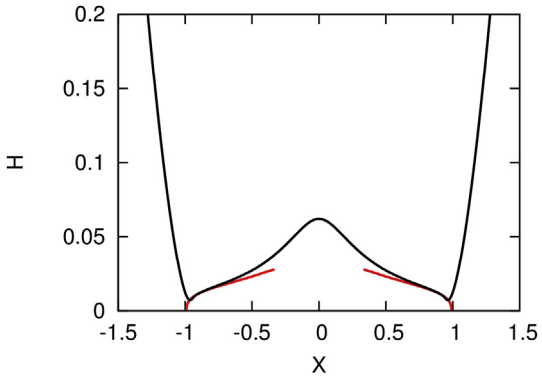

Fig. 3. Calculated film (black) and approximated (red). (For interpretation of the references to colour in this figure legend, the reader is referred to the Web version of this article.)

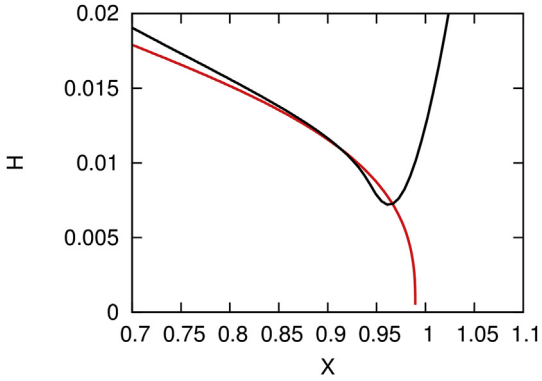

Fig. 4. Zoom of calculated film (black) and approximated (red). (For interpretation of the references to colour in this figure legend, the reader is referred to the Web version of this article.)

4. Amplitude reduction

In a rolling EHL contact the pressures are sufficiently large to generate large deformations of the solid surfaces, i.e. the EHL domain is also called ”piezo-viscous elastic”, where ”elastic” means that the elastic deformations are one or several orders of magnitude larger than the film thickness.

However, in the inlet boundary layer, surface roughness or surface waviness gives rise to local pressure variations, that can significantly alter the waviness amplitude. This waviness modification is defined by the amplitude reduction theory for line contacts [16,52] and for circular contacts [20,53]. These predictions were experimentally validated by Sperka et al. [54]. For a two dimensional isotropic waviness,

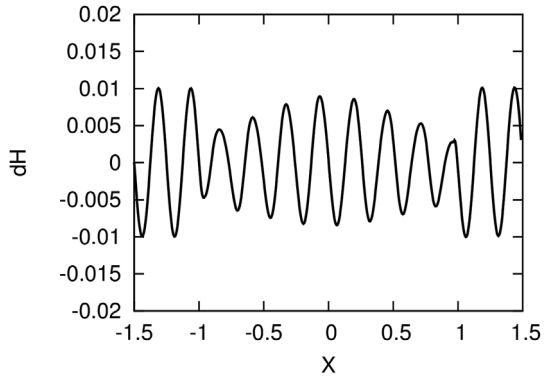

Fig. 5. Waviness amplitude over the contact at the moment of maximum impact.

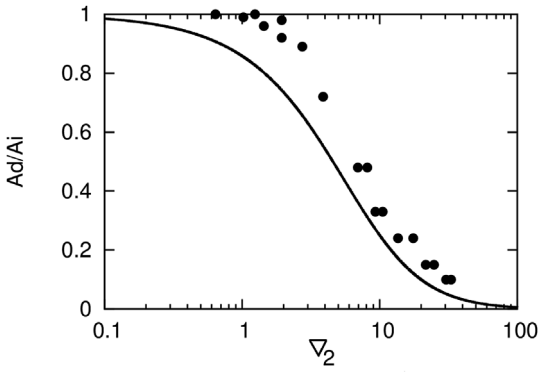

Fig. 6. Impact waviness amplitude reduction (dots) versus prediction (solid line).

the waviness deformation is given by:

$$\frac{A_d}{A_i} = \frac{1}{1 + 0.15\nabla_2 + 0.015\nabla_2^2} \tag{15}$$

$$\nabla_2 = \frac{\lambda}{a}\sqrt{\frac{M}{L}} = \frac{\lambda}{a}\frac{2}{\sqrt{\bar{\alpha}\bar{\lambda}}} \tag{16}$$

In a classical rolling contact the definition of the waviness amplitude is simple: observe the film thickness at a fixed position ($X = 0$) and monitor the maximum and the minimum film values. The deformed amplitude A_d is defined as $A_d = (H_{max_T} - H_{min_T})/2$.

Two additional difficulties appear in the impact contact problem: the waviness is frozen in (it does not change over time). The second difficulty is that the film thickness is not constant, but has a complicated shape. As such the amplitude reduction is defined by the first deformed waviness (completely inside the contact). Fig. 5 shows the computed waviness inside ($|X| < 1$) and outside ($|X| > 1$) the contact zone (H_{wavy}). At the moment of maximum impact, the waviness deformation is defined by:

$$dH(X, Y = 0) = H_{wavy}(X, Y = 0) - H_{smooth}(X, Y = 0) \tag{17}$$

The waviness deforms only a little in the center of the contact, whereas the deformation increases towards $|X| = 1$. By definition $A_d/A_i \to 0$ for $|X| \to 1$ as the boundary layer velocity tends to zero and $\nabla_2 \to \infty$!

As such the deformed amplitude is defined by the amplitude of the wave nearest to $|X| = 1$ at the moment of maximum impact. The local ∇_2 parameter is defined using $\bar{\lambda}$ times the local velocity.

Thus one can now plot the amplitude reduction curve A_d/A_i as a function of the local ∇_2 and the result is given in Fig. 6.

5. Conclusion

The current paper studies the point contact impact problem. It shows that the dimensionless Reynolds equation for the impact problem and the rolling sliding problem can be written in an identical way. The impact problem notation features an impact time $t_0 = \delta/v_0$, whereas the rolling/sliding problem uses the transit time $t_0 = a/u_m$. During impact the boundary layer velocity changes, giving rise to a complex bell-shaped film geometry. During a significant part of the impact the boundary velocity evolves linearly with time. It was shown that this linear velocity evolution linked with the classical relation $h \propto u^{0.67}$ allows for a good first order film shape prediction.

Finally, it was shown that the waviness inside an impacting contact deforms and that this deformation varies over the contact. Close to the contact centre the deformation is smallest, whereas it increases towards the contact periphery. The waviness deformation behaviour $A_d/A_i(\nabla_2)$ is similar to the trends observed in the rolling sliding contact. When including the local boundary layer velocity in the ∇_2 parameter, good quantitative agreement with the amplitude reduction theory was obtained.

Appendix

Johnson [28] gives an approximation of the Hertzian deformation δ as a function of time t, using t^* as the impact time.

$$\frac{\delta}{\delta^*} = \sin\left(\frac{\pi t}{2t^*}\right) \tag{18}$$

with an impact time $t \in [0,2t^*]$, however, it will be more convenient to use

$$\frac{\delta}{\delta^*} = \cos\left(\frac{\pi t}{2t^*}\right) \tag{19}$$

with an impact time $t \in [-t^*, t^*]$. The Hertzian deformation is linked to the contact radius a through $\delta = a^2/R_x$. As R_x is a constant we can write

$$\frac{a}{a^*} = \sqrt{\frac{\delta}{\delta^*}} = \sqrt{\cos\left(\frac{\pi t}{2t^*}\right)} \tag{20}$$

as we are interested in the contact radius around its maximum value, for t close to 0, we can use the Taylor expansion of order two

$$\frac{a}{a^*} = \sqrt{1 - \frac{\pi^2 t^2}{8t^{*2}}} \tag{21}$$

because of the Taylor expansion, the impact time is no longer $2t^*$ which can easily be remedied by removing the constants from the equation

$$\frac{a(t)}{a^*} = \sqrt{1 - \frac{t^2}{t^{*2}}} \tag{22}$$

by time derivation the velocity of the contact radius can be obtained

$$\frac{v(t)}{v^*} = \frac{-t/t^*}{\sqrt{1 - t^2/t^{*2}}} \tag{23}$$

For t close to zero, a linear relation between velocity and time is observed.

$$\frac{v(t)}{v^*} = \frac{-t}{t^*} \tag{24}$$

It is obvious that this simplification should be accurate around the time of maximum impact, $t = 0$, however, even around $|t| = t^*$ it closely approximates the asymptotically infinite velocities.

The impact time is given by Johnson as $t^* = 2.94$ and by Wijnant [55] as $t^* = 2.69$. The last value is closest to the $t^* = 2.7$ value observed in this work.

References

[1] Martin HM. Lubrication of gear theeth. Engineering 1916;vol. 102:199.
[2] Gümbel L. Uber geschmierte arbeitsräder. Z. Ges. Turbinenwesen 1916;13:357.
[3] Grubin AN, Vinogradova IE. Investigation of the contact of machine components. Moscow: Central ScientificResearch Institute for Technology and Mechanical Engineering; 1949. book 30, (DSIR translation 337).
[4] Petrusevitch AI. Fundamental conclusions from the contact hydrodynamic theory of lubrication. Izv. Akad. Naud. SSSR (OTN) 1951;2:209.
[5] Dowson D, Higginson GR. Elasto-hydrodynamic lubrication: the fundamentals of roller and gear lubrication. Pergamon Press; 1966.
[6] Hamrock BJ, Dowson D. Isothermal EHL of point contacts: fully flooded results. ASME Trans. JoLT 1976;99:264–77.
[7] Nijenbanning G, Venner CH, Moes H. Film thickness in elastohydrodynamically lubricated elliptic contacts. Wear 1991;176:217–29.
[8] Canzi A, Lubrecht AA, Venner CH. Film thickness predictions in elastohydrodynamically lubricated elliptical contacts. Proc IME J J Eng. Tribol. 2010;224(9):917–23. http://dx.doi.org/10.1243/13506501JET717.
[9] Lubrecht AA, Venner CH, Colin F. Film thickness calculation in elasto-hydrodynamic line and elliptical contacts: the Dowson, Higginson, Hamrock contribution. Proc IME J J Eng Tribol 2009;223(3):511–6. http://dx.doi.org/10.1243/13506501JET508.
[10] Venner CH, Lubrecht AA. Revisiting film thickness in slender EHL contacts. Proc IME J J Eng Tribol 2010;224:2549–58. http://dx.doi.org/10.1243/09544062JMES2316.
[11] Chevalier F, Lubrecht AA, Cann PME, Dalmaz G. Film thickness in starved EHL point contacts. ASME J Tribol 1998;120(1):126–33. http://dx.doi.org/10.1115/1.2834175.
[12] Popovici G, Venner CH, Lugt PM. Effects of load system dynamics on the film thickness in EHL contacts during start up. ASME J Tribol. 2004;126:258–66. http://dx.doi.org/10.1115/1.1645296.
[13] Venner CH, Wijnant YH. Validation of EHL contact predictions under time varying load. Proc IME J J Eng Tribol 2005;219:1–9. http://dx.doi.org/10.1243/135065005X33865.
[14] Venner CH, Hagmeijer R. Film thickness in EHL circular contacts under oscillatory speed conditions. Proc IME J J Eng Tribol 2008;222(4):533–48. http://dx.doi.org/10.1243/13506501JET306.
[15] Venner CH, Lubrecht AA. Numerical Simulation of a transverse ridge in a circular EHL contact under Rolling/Sliding. ASME J Tribol. 1994;116:751–61.
[16] Venner CH, Lubrecht AA. Numerical analysis of the influence of waviness on the film thickness of a circular EHL contact. ASME J Tribol. 1995;118:153–61.
[17] Zhu D, Hu Y-Z. A computer program package for the prediction of EHL and mixed lubrication characteristics, friction, subsurface stresses and flash temperatures based on measured 3-d surface roughness. Tribol Trans 2001;44(3):383–90. http://dx.doi.org/10.1080/10402000108982471.
[18] Greenwood JA, Johnson KL. The behaviour of transverse roughness in sliding elastohydrodynamically lubricated contacts. Wear 1992;153(1):107–17. http://dx.doi.org/10.1016/0043-1648(92)90264-9.
[19] Venner CH, Couhier F, Lubrecht AA, Greenwood J. Amplitude reduction of waviness in transient EHL line contacts. In: Dowsoneditor. Proceedings of the 1996 leeds-lyon conference, leeds, September 1996. 1997. p. 103–12.
[20] Venner CH, Lubrecht AA. An engineering tool for the quantitative prediction of general roughness deformation in EHL contacts based on harmonic waviness attenuation. Proc IME J J Eng Tribol 2005;219:303–12. http://dx.doi.org/10.1243/135065005X3397 Special Issue.
[21] Hooke CH, Venner CH. Surface roughness attenuation in line and point contacts. MechE J Eng Tribol 2000;214(J5):439–44. http://dx.doi.org/10.1243/1350650001543313.
[22] Morales-Espejel GE, Venner CH, Greenwood JA. Kinematics of transverse real roughness in EHL line contacts using fourier analysis. Proc IME J J Eng Tribol 2000:523–34. http://dx.doi.org/10.1243/1350650001543395.
[23] Venner CH, Hooke CJ. Surface roughness attenuation in EHL line and point contacts under conditions of starved lubrication. Snidle RW, Evans HP, editors. Proc. IUTAM symposium on elastohydrodynamics and micro-elastohydrodynamics, vol. 134. Springer series Solid Mechanics and its Applications; 2005. p. 59–70.
[24] Cann PM, Spikes HA, Hutchinson J. The development of a spacer layer imaging method (SLIM) for mapping elastohydrodynamic contacts. Tribol Trans 1996;39(4):915–21.
[25] Dowson D, Ehret P. Past, present and future studies in elastohydrodynamics. Proc IME J J Eng Tribol 1999;213(5):317–33. http://dx.doi.org/10.1243/1350650991542703.
[26] Spikes HA. Sixty years of EHL. Lubric Sci 2006;18(4):265–91.
[27] Lugt PM, Morales-Espejel GE. A review of elasto-hydrodynamic lubrication theory. Tribol Trans 2011;54(3):470–96. http://dx.doi.org/10.1080/10402004.2010.551804.
[28] Johnson KL. Contact mechanics. Cambridge University Press; 1985.
[29] Christensen H. Elastohydrodynamic theory of spherical bodies in normal approach. ASME J Lubric Technol 1970;92:145–54.
[30] Yang PR, Wang SZ. Pure squeeze action in an isothermal elastohydrodynamically spherical conjunction, part 1: theory and dynamic load results. Wear 1991;142:1–16.
[31] Larsson R, Höglund E. Numerical simulation of a ball impacting and rebounding a lubricated surface. ASME J Lubric Technol 1994;116:770–6.
[32] Guo F, Kaneta M, Wang J. Occurrence of a noncentral dimple in squeezing EHL contacts. ASME J Lubric Technol 2006;128:632–40.
[33] Kaneta M, Guo F, Wang J. Impact micro-elastohydrodynamics in point contacts. ASME J Lubric Technol 2011;133:1–9. pp. (031503).
[34] Kaneta M, Guo F, Wang J, Krupka I, Hartl M. Pressure increase in elliptical impact elastohydrodynamic lubrication contacts with longitudinal asperities. J Tribol 2012;135(1):011503. http://dx.doi.org/10.1115/1.4007808/.
[35] Kaneta M, Nishikawa H, Mizui M, Guo F. Impact elastohydrodynamics in point contacts. Proc IME J J Eng Tribol 2016;225(1):1–12. http://dx.doi.org/10.1177/13506501JET838.
[36] Paul GR, Cameron A. An Absolute high-pressure microviscometer based on refractive index. Proc. Roy. Soc. London, Series A 1972;331:171–84.
[37] Safa MMA, Gohar R. Pressure distribution under a ball impacting a thin lubricant layer. ASME J Tribol 1986;108:372–6.
[38] Wong PL, Lingard S, Cameron A. The high-pressure impact viscometer. Tribol Trans 1992;35:500–8.
[39] Kaneta M, Ozaki S, Nishikawa H, Guo F. Effects of impact loads on point contact elastohydrodynamic lubrication films. Proc IME J J Eng Tribol 2007;221:271–8.
[40] Nishikawa H, Miyazaki H, Kaneta M, Guo F. Effects of two-stage impact load on point contact elastohydrodynamic lubrication films. Proc IME J J Eng Tribol 2008;222:807–14. http://dx.doi.org/10.1243/13506501JET389.
[41] Visser CW, Frommhold PE, Wildeman S, Mettin R, Lohse D, Sun C. Dynamics of high-speed micro-drop impact: numerical simulations and experiments at frame- to-frame times below 100 ns. Soft Matter 2015;11(9):1708–22.
[42] Wang J, Venner CH, Lubrecht AA. Central film thickness prediction for line contacts under pure impact vol. 66. Elsevier, Tribology International; 2013. p. 203–7.
[43] Venner CH, Wang J, Lubrecht AA. Central film thickness in EHL Point Contacts under Pure Impact Revisited vol. 100. Elsevier, Tribology International; 2016. p. 1–6.
[44] Snoeijer JH, Eggers J, Venner CH. Similarity theory of lubricated Hertzian contacts. Phys Fluids 2013;25:101705.
[45] Venner CH, Biboulet N, Lubrecht AA. Boundary layer behaviour in circular EHL contacts in the elastic-piezo-viscous regime. Tribol Lett 2014;56(2):375–86.
[46] Biboulet N, Lubrecht AA. On boundary layers and pressure spikes, a tribute to J.-M. Georges. Bearing World, 2016 2016;1:61–74.
[47] Moes H, Bosma R. Optimum similarity analysis, an application to

elastohydrodynamic lubrication. Wear 1992;159:57–66.
[48] Moes H. Lubrication and beyond. 2000 available from the University of Twente web-site www.utwente.nl/ctw/tr/Organisation/Links/Moes.pdf.
[49] Roelands CWA. Correlational aspects of the viscosity-temperature-pressure relationship of lubricating oils PhD thesis the Netherlands: Technische Hogeschool Delft; 1966.
[50] Venner CH, Lubrecht AA. Multilevel methods in lubrication. Elsevier; 2000.
[51] Wijnant YH, Venner CH. Analysis of an EHL circular contact incorporating rolling element vibration. In: Dowson D, editor. Proceedings of the 1996 Leeds-Lyon. Leeds, England. 1997. p. 445–56.
[52] Lubrecht AA, Graille D, Venner CH, Greenwood JA. Waviness deformation in EHL line contacts under rolling/sliding. ASME JoT 1997;120:705–9.
[53] Lubrecht AA, Venner CH. Elastohydrodynamic lubrication of rough surfaces. Proc Inst Mech Eng Part J 1999;213:397–404.
[54] Sperka P, Krupka I, Hartl M. Experimental study of real roughness attenuation in concentrated contacts. Tribol Int 2010;43. 1893âĂŞ1901.
[55] Wijnant YH. Contact dynamics in the field of elastohydrodynamic Lubrication PhD thesis University Twente; 1998